

## Case Report

Spinal cord anaplastic astrocytoma with *BRAF* V600E mutation: A case report and review of literatureSoichiro Takamiya,<sup>1</sup>  Kanako C. Hatanaka,<sup>2</sup> Yukitomo Ishi,<sup>1</sup>  Toshitaka Seki<sup>1</sup> and Shigeru Yamaguchi<sup>1</sup><sup>1</sup>Department of Neurosurgery, Faculty of Medicine and Graduate School of Medicine, Hokkaido University and <sup>2</sup>Department of Surgical Pathology, Hokkaido University Hospital, Sapporo, Japan

**A 17-year-old female complained of lower extremity pain that progressed to low back pain accompanied by paraparesis. Magnetic resonance imaging revealed a mass in the conus medullaris of the spinal cord at the thoracic spine 11–12 level. The patient underwent resection of the mass. The pathological diagnosis was anaplastic astrocytoma based on the densely proliferating astrocytic tumor cells without necrosis or microvascular proliferation. The patient received chemoradiotherapy with oral temozolomide and a total of 54 Gy of local irradiation, followed by 24 courses of temozolomide as maintenance chemotherapy. The patient survived for 8 years without tumor recurrence following the initial treatment. Genetic analysis of the tumor revealed a *BRAF* V600E mutation that has not yet been reported in spinal cord high-grade gliomas (HGGs). In recent years, the molecular therapy targeting the *BRAF* V600E mutation has been applied in clinical practice for several cancer types. Although the frequency in spinal cord HGGs is uncertain, it is necessary to investigate *BRAF* V600E mutation as a potential therapeutic target in the future.**

**Key words:** anaplastic astrocytoma, *BRAF* V600E mutation, spinal cord high-grade glioma.

## INTRODUCTION

B-type Raf (*BRAF*) is a component of the mitogen-activated protein kinase (MAPK) pathway that regulates cell growth, proliferation, and differentiation.<sup>1,2</sup> The activation of mutations in *BRAF* cause abnormal cell growth, which can lead to tumorigenesis. A missense mutation in *BRAF* results in a change at codon 600 that substitutes

glutamine for valine (*BRAF* V600E), as detected in several types of low-grade gliomas (LGGs), including pleomorphic xanthoastrocytomas (PXAs), gangliogliomas (GGs), and supratentorial pilocytic astrocytomas (PAs).<sup>3</sup> In comparison, *BRAF* V600E mutation is rare in intracranial high-grade gliomas (HGGs), which account for 1.7%–6.3% of cases.<sup>3–6</sup> In spinal cord gliomas, *BRAF* alterations including the V600E mutation, copy number gain, and fusion are frequently detected in LGGs,<sup>7–9</sup> whereas the missense mutation resulting in the substitution of methionine for lysine at residue 27 of the H3 histone family member 3A (*H3F3A* K27M) is frequently detected in HGGs.<sup>7,9–12</sup> Although several cases of spinal cord LGGs harboring *BRAF* V600E mutations have been reported,<sup>5,13–16</sup> there has been no report of *BRAF* mutations in spinal cord HGGs. Here, we report a rare case of spinal cord anaplastic astrocytoma harboring a *BRAF* V600E mutation.

## CLINICAL SUMMARY

A 17-year-old female presented with lower extremity pain, which progressed to low back pain and paraparesis over 6 months. A lumbar magnetic resonance imaging (MRI) performed at the previous hospital revealed a mass in the conus medullaris of the spinal cord; therefore, the patient was transferred to our department for further management. Neurological examinations revealed paraparesis (grade III in manual muscle testing on bilateral lower extremities) and hyperactive deep tendon reflexes in the right ankle and plantar. The lumbar MRI revealed an intramedullary tumor at the thoracic 11–12 (T11–T12) level (Fig. 1A–D). The tumor was located on the left side of the conus medullaris. It showed mixed hyperintensity on T2-weighted image and isointensity on T1-weighted image as well as was heterogeneously enhanced with gadolinium contrast medium. The patient underwent a tumor resection via laminectomy at the T11–T12 level. Because the tumor was not well circumscribed, the surgery achieved a partial resection, and the postoperative MRI

Correspondence: Yukitomo Ishi, Department of Neurosurgery, Hokkaido University Graduate School of Medicine, North 15 West 7, Kita-ku, Sapporo 060-8638, Japan. Email: ishi-y@huhp.hokudai.ac.jp

Received 15 October 2019; accepted 06 November 2019.

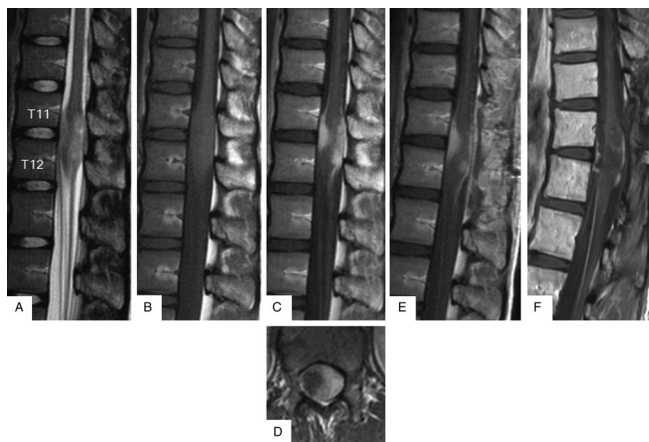


**Fig. 1** Findings obtained from the lumbar spinal cord. The MRI reveals an intradural tumor at the thoracic spine 11–12 level. The tumor shows mixed hyperintensity on T2-weighted image (A) and iso-intensity on T1-weighted image (B) as well as being heterogeneously enhanced with gadolinium contrast medium (C). The axial image shows the tumor located at the left side of the conus medullaris (D). The postoperative MRI taken after the surgery reveals no significant change in the enhanced lesion as compared with that before surgery (E). However, MRI taken 8 years after the initial treatment shows no evidence of residual tumor except the postoperative changes after 24 courses of temozolomide as maintenance chemotherapy (F).

revealed residual tumor (Fig. 1E). Following the surgery, the patient's leg pain improved and no other symptom occurred. Under the pathological diagnosis of anaplastic astrocytoma (World Health Organization (WHO) grade III), the patient underwent chemotherapy with oral temozolomide (75 mg/m<sup>2</sup>/day) and local irradiation with an overall dose of 54 Gy in 27 fractions. This was followed by 24 courses of temozolomide as maintenance chemotherapy. The size of the residual tumor decreased during the maintenance chemotherapy. The patient has survived for 8 years without recurrence following the initial treatment (Fig. 1F).

## HISTOPATHOLOGICAL FINDINGS

Hematoxylin and eosin (HE) staining of the surgical specimens demonstrated densely proliferating tumor cells with swollen nuclei and eosinophilic cytoplasmic processes (Fig. 2A). No evidence of necrosis, microvascular proliferation, or epithelioid cells was observed. The immunohistochemical staining of tumor cells was positive for glial fibrillary acidic protein (GFAP) (Fig. 2B). The Ki-67 labeling index was approximately 10% (Fig. 2C).

## GENETIC ANALYSIS

Genomic DNA was extracted from the formalin-fixed, paraffin-embedded (FFPE) tumor samples using ReliaPrep™ FFPE gDNA Miniprep System (Promega, Madison, WI, USA), according to the manufacturer's

instructions. Two mutation hotspots within the telomerase reverse transcriptase gene (*TERT*) promoter—C228T and C250T—along with mutation hotspots at codon 132 of the isocitrate dehydrogenase 1 gene (*IDH1*), codon 172 of *IDH2*, codons 27 and 34 of the H3 histone family member 3A gene (*H3F3A*), codon 27 of the histone cluster 1 H3 family member B gene (*HIST1H3B*), and codon 600 of *BRAF* were screened using Sanger sequencing. Genomic DNA was amplified via polymerase chain reaction (PCR) using AmpliTaq Gold® (Thermo Fisher Scientific, MA, USA) for the *TERT* promoter and Quick Taq® HS DyeMix (TOYOBO, Osaka, Japan) for other genes. The oligonucleotide primers used for amplification are shown as follows: forward (F) (5'-CAGGACCGCGCTTCCCAC-3') and reverse (R) (5'-AGCGCTGCCTGAAACTCG-3') for *TERT* promoter (first), F (5'-CACGTGGCGGAGGGACTG-3') and R (5'-AGCGCTGCCTGAAACTCG-3') for *TERT* promoter (nested), F (5'-TGTGGAAATCACCAAATGGCAC-3') and R (5'-TACAAGTTGGAAATTTCTGGGC-3') for *IDH1*, F (5'-GGGAGCCCATCATCTGCAAAAA-3') and R (5'-ACAAGAGGATGGCTAGGCGA-3') for *IDH2*, F (5'-TCAATGCTGGTAGGTAAGTAAGGA-3') and R (5'-GGTTTCTTCACCCCTCAGT-3') for *H3F3A*, F (5'-TCGTAATAAACAGACAGCTCGG-3') and R (5'-CGGTAACGGTGAGGCTTTTT-3') for *HIST1H3B*, and F (5'-TGCTTGCTCTGATAGGAAAATG3') and R (5'-TGATGGGACCCACTCCAT-3') for *BRAF*. Cycle sequencings were performed with the BigDye Terminator v3.1 Cycle Sequencing Kit (Applied Biosystems, Foster City, CA, USA) using the F and R PCR primers as sequencing primers.

Among the genes screened, the tumor presented a *BRAF* V600E mutation (Fig. 2D). *TERT* promoter, *IDH1/2*, *H3F3A*, and *HIST1H3B* were wild-type.

## DISCUSSION

To the best of our knowledge, this is the first case of a spinal cord HGG harboring *BRAF* V600E mutation. *BRAF* V600E mutation is commonly detected in malignant melanomas and colorectal, ovarian, and papillary thyroid carcinomas.<sup>2</sup> With regard to the neoplasms of the central nervous system, *BRAF* V600E mutation is frequently detected in LGGs but rarely in HGGs. Schindler et al. reported high frequencies of *BRAF* V600E mutations in PXAs (66%), GGs (18%), and extra-cerebellar PAs (9%) in an analysis of 1320 nervous system tumors.<sup>5</sup> Although high frequencies of *BRAF* V600E mutation in epithelioid glioblastoma—a rare variant of glioblastoma with an epithelioid feature in pathology—have been reported,<sup>6,17,18</sup> a limited number of HGGs have been detected harboring this mutation.<sup>3–6,19,20</sup>

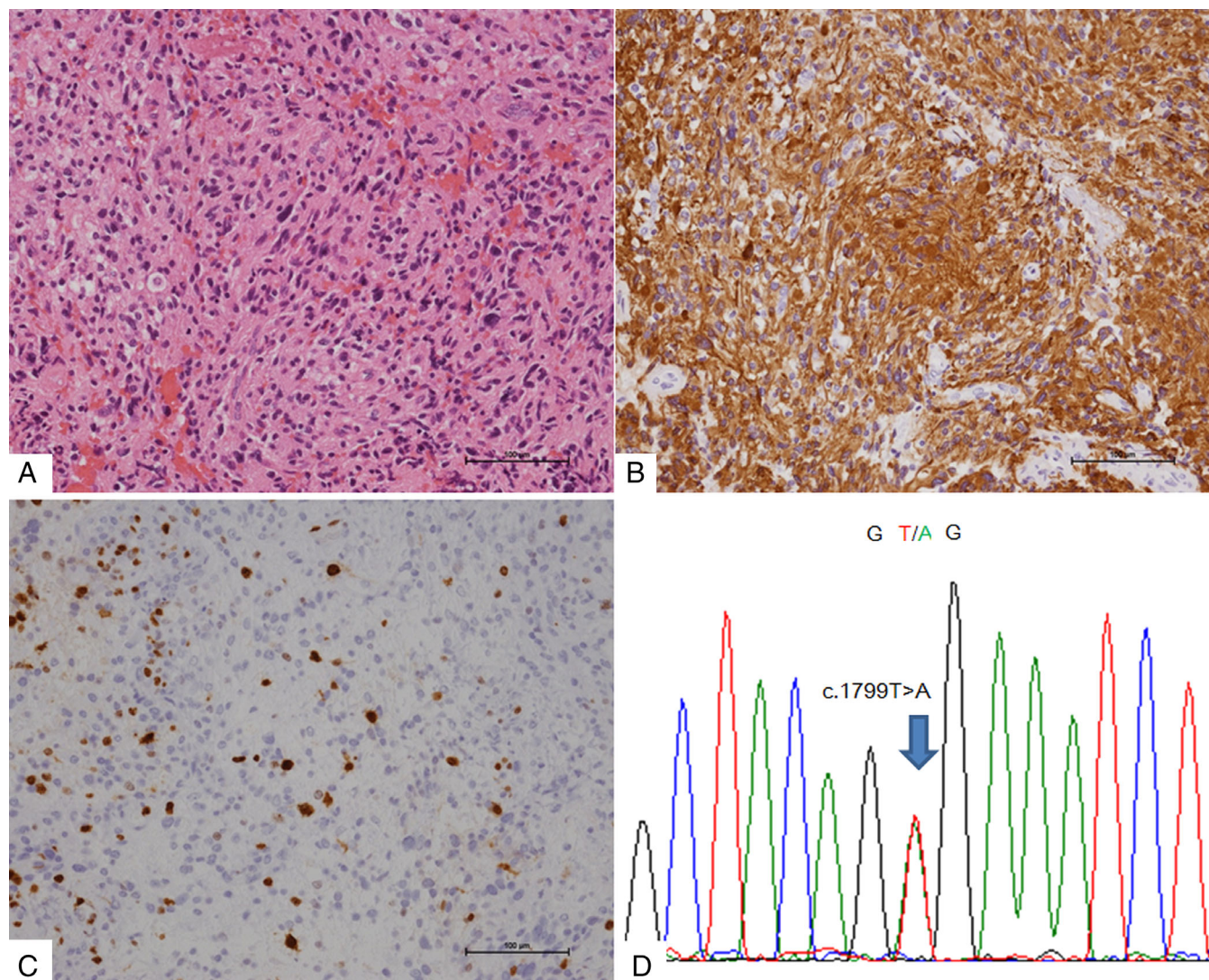


**Fig. 2** Histopathological findings and genetic analysis. HE staining shows densely proliferating tumor cells with swollen nuclei and eosinophilic cytoplasmic processes (A). Immunohistochemical staining shows that the tumor cells are positive for GFAP (B). The Ki-67 labeling index is approximately 10% (C). DNA sequencing of *BRAF* reveals a thymine-to-adenine substitution at nucleotide 1799, indicating *BRAF* V600E mutation (arrow) (D).

In spinal cord gliomas, *BRAF* alterations including the copy number gain of *BRAF* or *BRAF-KIAA1549* fusion that activate MAPK signaling are frequently detected in LGGs (WHO grades I and II),<sup>7</sup> whereas the *H3F3A* K27M mutation is frequently detected in HGGs (WHO grades III and IV).<sup>7,10–12,21</sup> All of the reported spinal cord gliomas harboring *BRAF* V600E mutations are LGGs (Table 1).<sup>5,13–16</sup> Among the 24 cases of spinal cord HGGs investigated, none of them harbored *BRAF* V600E mutation (Table 2).<sup>7,10,12,22,23</sup> Hence, our case is the first report of a spinal cord HGG harboring *BRAF* V600E mutation.

Recently, molecular therapy targeting the *BRAF* V600E mutation has been applied in clinical practice for malignant melanomas and other types of malignant

**Table 1** Summary of previously reported *BRAF* V600E mutations in spinal cord gliomas

Authors and year	Pathology	Age	Gender	Location
Schindler, 2001 <sup>5</sup>	PA	ND	ND	ND
Gessi, 2016 <sup>13</sup>	GG	9	M	MO-C6
	GG	8	M	C7-Th2
Hong, 2017 <sup>14</sup>	PXA	31	M	Th12-L1
Pages, 2018 <sup>15</sup>	GG	11	M	ND
	GG	14	F	ND
Garnier, 2019 <sup>16</sup>	GG	22	M	C3-5

C, cervical; F, female; GG, ganglioglioma; L, lumbar; M, male; MO, medulla oblongata; ND, not described; PA, pilocytic astrocytoma; PXA, pleomorphic xanthoastrocytoma; Th, thoracic.

**Table 2** Summary of the previously reported analyses of *BRAF* V600E in spinal cord high-grade gliomas

Authors and year	Analysis method	Frequency of <i>BRAF</i> V600E mutation
Solomon, 2015 <sup>12</sup>	IHC	0/4
Liu, 2015 <sup>22</sup>	IHC	0/1
Shankar, 2016 <sup>7</sup>	Seq	0/4
Nagaishi, 2016 <sup>23</sup>	Seq	0/2
Alvi, 2019 <sup>10</sup>	IHC + Seq	0/13

IHC, immunohistochemistry; Seq, sequencing.

tumors.<sup>24</sup> For intracranial HGGs, the efficacy of *BRAF* inhibitors has been reported in laboratory and clinical studies.<sup>25–28</sup> Although genetic analysis has been performed in several cases of spinal cord HGGs, most reports did not describe the *BRAF* V600E.<sup>11,21,29</sup> Therefore, the frequency of *BRAF* V600E mutation in spinal cord HGGs remains unclear. However, as elucidated from this case, genetic analysis for *BRAF* V600E mutation in spinal cord HGGs would be necessary, considering the potential for identifying a molecular targeted therapy. In conclusion, we reported the rare case of spinal cord anaplastic astrocytoma harboring a *BRAF* V600E mutation. This is the first case of a *BRAF* V600E mutation detected in a spinal cord HGG. Although the frequency in spinal cord HGGs is uncertain, we consider that it is necessary to investigate *BRAF* V600E mutation as a potential therapeutic target in the future.

## DISCLOSURE

The authors declare that they have no conflict of interest.

## REFERENCES

- Davies H, Bignell GR, Cox C *et al.* Mutations of *BRAF* gene in human cancer. *Nature* 2002; **417**: 949–954.
- Wan PT, Garnett MJ, Roe SM *et al.* Mechanism of activation of the RAF-ERK signaling pathway by oncogenic mutations of B-RAF. *Cell* 2002; **116**: 855–867.
- Park CK, Lee SH, Kim JY *et al.* Expression level of hTERT is regulated by somatic mutation and common single nucleotide polymorphism at promoter region in glioblastoma. *Oncotarget* 2014; **5**: 3399–3407.
- Arita H, Yamasaki K, Matsushita Y *et al.* A combination of TERT promoter mutation and MGMT methylation status predicts clinically relevant subgroups of newly diagnosed glioblastomas. *Acta Neuropathol Commun* 2016; **4**: 79.
- Schindler G, Capper D, Meyer J *et al.* Analysis of *BRAF* V600E mutation in 1,320 nervous system tumors reveals high mutation frequencies in pleomorphic xanthoastrocytoma, ganglioglioma and extra-cerebellar pilocytic astrocytoma. *Acta Neuropathol* 2011; **121**: 397–405.
- Hatae R, Hata N, Suzuki SO *et al.* A comprehensive analysis identifies *BRAF* hotspot mutations associated with gliomas with peculiar epithelial morphology. *Neuropathology* 2017; **37**: 191–199.
- Shankar GM, Lelic N, Gill CM *et al.* *BRAF* alteration at status and the histone H3F3A gene K27M mutation segregate spinal cord astrocytoma histology. *Acta Neuropathol* 2016; **131**: 147–150.
- Collins VP, Jones DT, Giannini C. Pilocytic astrocytoma: Pathology, molecular mechanisms and markers. *Acta Neuropathol* 2015; **129**: 775–788.
- Johnson A, Severson E, Gay L *et al.* Comprehensive genomic profiling of 282 pediatric low- and high-grade gliomas reveals genomic drivers, tumor mutational burden, and hypermutation signatures. *Oncologist* 2017; **22**: 1478–1490.
- Alvi MA, Ida CM, Paolini MA *et al.* Spinal cord high-grade infiltrating gliomas in adults: Clinicopathological and molecular evaluation. *Mod Pathol* 2019; **32**: 1236–1243.
- Gessi M, Gielen GH, Dreschmann V, Waha A, Pietsch T. High frequency of H3F3A (K27M) mutations characterizes pediatric and adult high-grade gliomas of the spinal cord. *Acta Neuropathol* 2015; **130**: 435–437.
- Solomon DA, Wood MD, Tihan T *et al.* Diffuse midline gliomas with histone H3-K27M mutation: A series of 47 cases assessing the spectrum of morphologic variation and associated genetic alterations. *Brain Pathol* 2016; **26**: 569–580.
- Gessi M, Dorner E, Dreschmann V *et al.* Intramedullary gangliogliomas: Histopathologic and molecular features of 25 cases. *Hum Pathol* 2016; **49**: 107–113.
- Hong CS, Wang JL, Dornbos DIII, Joehlin-Price A, Elder JB. *BRAF*-mutated pleomorphic xanthoastrocytoma of the spinal cord with eventual anaplastic transformation. *World Neurosurg* 2017; **98**: 871 e9-15.
- Pages M, Beccaria K, Boddaert N *et al.* Co-occurrence of histone H3 K27M and *BRAF* V600E mutations in paediatric midline grade I ganglioglioma. *Brain Pathol* 2018; **28**: 103–111.
- Garnier L, Ducray F, Verlut C *et al.* Prolonged response induced by single agent vemurafenib in a *BRAF* V600E spinal ganglioglioma: A case report and review of the literature. *Front Oncol* 2019; **9**: 177.

17. Behling F, Barrantes-Freer A, Skardelly M *et al.* Frequency of BRAF V600E mutations in 969 central nervous system neoplasms. *Diagn Pathol* 2016; **11**: 55.
18. Kleinschmidt-DeMasters BK, Aisner DL, Birks DK, Foreman NK. Epithelioid GBMs show a high percentage of BRAF V600E mutation. *Am J Surg Pathol* 2013; **37**: 685–698.
19. Suzuki Y, Takahashi-Fujigasaki J, Akasaki Y *et al.* BRAF V600E-mutated diffuse glioma in an adult patient: A case report and review. *Brain Tumor Pathol* 2016; **33**: 40–49.
20. Nakata S, Horiguchi K, Ishiuchi S *et al.* A case of high-grade astrocytoma with BRAF and ATRX mutations following a long-standing course over two decades. *Neuropathology* 2017; **37**: 351–357.
21. Wang L, Li Z, Zhang M *et al.* H3 K27M-mutant diffuse midline gliomas in different anatomical locations. *Hum Pathol* 2018; **78**: 89–96.
22. Liu A, Sankey EW, Bettegowda C, Burger PC, Jallo GI, Groves ML. Poor prognosis despite aggressive treatment in adults with intramedullary spinal cord glioblastoma. *J Clin Neurosci* 2015; **22**: 1628–1631.
23. Nagaishi M, Nobusawa S, Yokoo H *et al.* Genetic mutations in high grade gliomas of the adult spinal cord. *Brain Tumor Pathol* 2016; **33**: 267–269.
24. Planchard D, Besse B, Groen HJM *et al.* Dabrafenib plus trametinib in patients with previously treated BRAFV600E-mutant metastatic non-small cell lung cancer: An open-label, multicentre phase 2 trial. *Lancet Oncol* 2016; **17**: 984–993.
25. Robinson GW, Orr BA, Gajjar A. Complete clinical regression of a BRAF V600E-mutant pediatric glioblastoma multiforme after BRAF inhibitor therapy. *BMC Cancer* 2014; **14**: 258.
26. Dasgupta T, Olow AK, Yang X *et al.* Survival advantage combining a BRAF inhibitor and radiation in BRAF V600E-mutant glioma. *J Neurooncol* 2016; **126**: 385–393.
27. Kaley T, Touat M, Subbiah V *et al.* BRAF inhibition in BRAF V600-mutant gliomas: Results from the VE-BASKET study. *J Clin Oncol* 2018; **36**: 3477–3484.
28. Toll SA, Tran HN, Cotter J *et al.* Sustained response of three pediatric BRAF V600E mutated high-grade gliomas to combined BRAF and MEK inhibitor therapy. *Oncotarget* 2019; **10**: 551–557.
29. Yi S, Choi S, Shin DA *et al.* Impact of H3.3 K27M mutation on prognosis and survival of grade IV spinal cord glioma on the basis of new 2016 World Health Organization classification of the central nervous system. *Neurosurgery* 2019; **84**: 1072–1081.